Density functional study of hydrogen adsorption on beryllium (0001)

A. Allouche*

Physique des Interactions Ioniques et Moléculaires, CNRS and Université de Provence, Campus Scientifique de Saint Jérôme, service 242, 13397 Marseille Cedex 20, France

(Received 9 May 2008; revised manuscript received 29 July 2008; published 22 August 2008)

Beryllium, tungsten, and carbon are planned as wall materials for the future international tokamak. Although beryllium is not situated in a region submitted to the most dramatic plasma-wall interaction, its reactivity toward hydrogen atom impinging is of fundamental importance. This paper is devoted to theoretical study of hydrogen adsorption on the beryllium (0001) surface based on the first-principles discrete Fourier transform method. Comparison is proposed to former theoretical works and to thermal-desorption spectroscopy.

DOI: 10.1103/PhysRevB.78.085429 PACS number(s): 71.15.Mb, 68.43.−h, 28.52.Fa, 52.55.Fa

I. INTRODUCTION

In a tokamak[1] the deuterium (D)-tritium (T) plasma is magnetically confined in order to reach energy and concentration high enough to induce the thermonuclear fusion of the two nuclei, thus releasing a very large amount of energy:

$$\mathrm{D} + \mathrm{T} \rightarrow \mathrm{He}(3.5\ \mathrm{MeV}) + n(14.1\ \mathrm{MeV}).$$

International thermonuclear experimental reactor (ITER) is an international research tokamak proposal, which is intended as an experimental project of magnetic confinement for future power generation through thermonuclear fusion.

Although the inner wall of ITER will be isolated from the hot plasma by confinement in magnetic fields, the wall will be still subjected to atom and ion fluxes issued from the boundary plasma. Therefore, the wall cladding is made up of materials of specific mechanical, magnetic, thermal, and electric properties: the largest part (690 m^2) of ITER's first wall will be constituted of beryllium. Its usefulness is based on its low atomic number, its ability to remove oxygen from the plasma through chemical reaction, and its ability to pump hydrogen during short discharges.[2] Beryllium is also considered a neutron multiplier.[3]

The problem of hydrogen trapping in graphite-based cladding of ITER inner walls has been extensively studied experimentally as well as by quantum modeling methods.[4] On the contrary, the beryllium behavior toward hydrogen is far from well investigated.[5] Experimental simulations have been proposed recently, notably by the Doerner[6] and the Reinelt and Linsmeier[7] groups.

Curiously, in another domain, beryllium is also considered as a good candidate for hydrogen storage in fuel cells and internal combustion engines, and in energy-conversion devices.[8] Actually, solid beryllium hydride has been used as a rocket fuel.[9] Therefore these dual and opposed properties of the material need special attention.

A few quantum studies have been published during the two last decades on hydrogen adsorption on beryllium. Marino and Ermler[10] proposed an *ab initio* Hartree-Fock calculation on a rigid Be_{45} cluster. One of the earlier periodic calculation made use of linearized augmented-plane-wave (LAPW) method[11] and was supplemented later by a first-principles calculations of the same group.[12] R. Stumpf[13] devoted his contribution to hydrogen mobility and defect formation. Very recently, Hector *et al.*[14] gave a systematic investigation of the alkaline earth hydrides: lattice parameters, electronic and vibrational energies, based on density-functional theory.

The aim of this work is to contribute in understanding the fundamental processes underlying hydrogen retention (and also restitution) by beryllium-based materials. These processes can only be completely elucidated through quantum theory and periodic (boundary conditions) first-principles density-functional theory (DFT) investigations since the metal cannot be reduced efficiently to a simple cluster of a few atoms. Since the first interface in a tokamak between the deuterium plasma and Be is the crystal surface, the first task is to study hydrogen adsorption; retention in the bulk will be considered elsewhere. How many atoms can be trapped on the surface? What is the cost in energy to remove them? What are the mechanisms of restitution? Quantum calculations provide a special answer to these questions.

The paper is organized as follows: The computational details are given in the Sec. II; they are very similar to those carried out in our former contribution.[15] Besides the usual practical parameters such as energy cutoff or Brillouin zone sampling used in this application, the beryllium pseudopotential is detailed and compared to all-electron calculations. Section III is devoted to single hydrogen atom interaction with beryllium surface, and then, to complete hydrogenation of the Be(0001) basal plane. A general discussion is given in the Sec. IV with comparison to previous experimental and theoretical works.

II. COMPUTATIONAL SECTION

The calculations were performed within the framework of the spin-polarized gradient-corrected DFT. All the computation runs started with spin-up polarized hydrogen atoms (according to the QUANTUM ESPRESSO terminology), and ended in zero-magnetization states, and spin-up and spin-down degenerated eigenstates. This means that the hydrogen electrons have been equally distributed on the metal energy bands. The exchange, as well as the correlation, functionals are Perdew-Burke-Ernzerhof (PBE). A plane-wave basis set was used with an energy cutoff of 32 Ry (435 eV); the ionic core potential was modeled using Vanderbilt ultrasoft pseudopotentials. Integration in the first Brillouin zone was

performed using the $6\times6\times1$ points Monkhorst-Pack sampling. In the following, the acronym PBE-PW stands for the combination PBE functional+plane-wave basis set.

The Be(0001) basal plane is represented by a 3×3 hexagonal supercell and a slab of five layers (45 Be atoms).

The interaction energy of n hydrogen atoms with a beryllium slab is defined as

$$\Delta E = [E(\mathrm{Be}+n\mathrm{H}) - E(\mathrm{Be}) - nE(\mathrm{H})]/n, \qquad (1)$$

where $E(\mathrm{Be}+n\mathrm{H})$ represents the total system energy, $E(\mathrm{Be})$ the Be slab energy in the same geometry, and $E(\mathrm{H})$ the energy of a single H atom calculated in the same unit cell.

The stationary-state structures were optimized using the Quasi-Newton Broyden-Fletcher-Goldfarb-Shanno generalized algorithm implemented in the QUANTUM ESPRESSO package.[16] All the atoms were included in the optimization procedure without any constraint. The hydrogen pseudopotential is taken from the package's library. The beryllium one is homemade; therefore we have to perform a series of tests, above all, because this atom has a very special electronic structure: with the two valence electrons on the $2s$ shell, Be can adopt some behavior of the helium atom with a very low dissociation energy of the dimer and long interatomic distance.

The PBE Vanderbilt ultrasoft pseudopotential we optimized for the beryllium yields the same dimer energy profile than the all-electron PBE [Fig. 1(a)]. The resulting crystal parameters (close-packed hexagonal structure) are in reasonable agreement with experiment: $\boldsymbol{a}=\boldsymbol{b}=2.28$ Å [experimental 2.29 Å (Ref. 17) other generalized gradient approximation (GGA) 2.26 Å (Ref. 14)] and $\boldsymbol{c}/\boldsymbol{a}=1.54$ (exp: 1.57; other GGA: 1.58). The cohesive energy is calculated as the difference between the total energy and the energy of a free atom in a cubic cell of box length=5 Å, its value being 3.7 eV. Therefore, PBE slightly overestimates (~0.4 eV) the cohesive energy but the results are in good agreement with previous DFT results.[14,18,19] The framework of this contribution cannot be more than semiquantitative, given the method and the sizes of the systems we are working with, and then this approximation looks sufficient.

To end with the problem of Be pseudopotential since this contribution deals with beryllium-hydrogen interaction, Fig. 1(b) shows clearly that, in the domain we are interested in (0–3 Å), the PBE-PW Vanderbilt pseudopotential method gives results in very good agreement with high level all-electron quantum methods, excepting that the PBE-PW curve exhibits a small maximum (~0.2 eV) around 3.8 Å. However, due to the well-known bad behavior of DFT at long distance, this cannot be considered as significant. The important point remains that the bond lengths at minimum are identical, and that the discrepancy between PBE-PW and CCSD(T) is only 0.08 eV; therefore the following calculations are developed within this approximation.

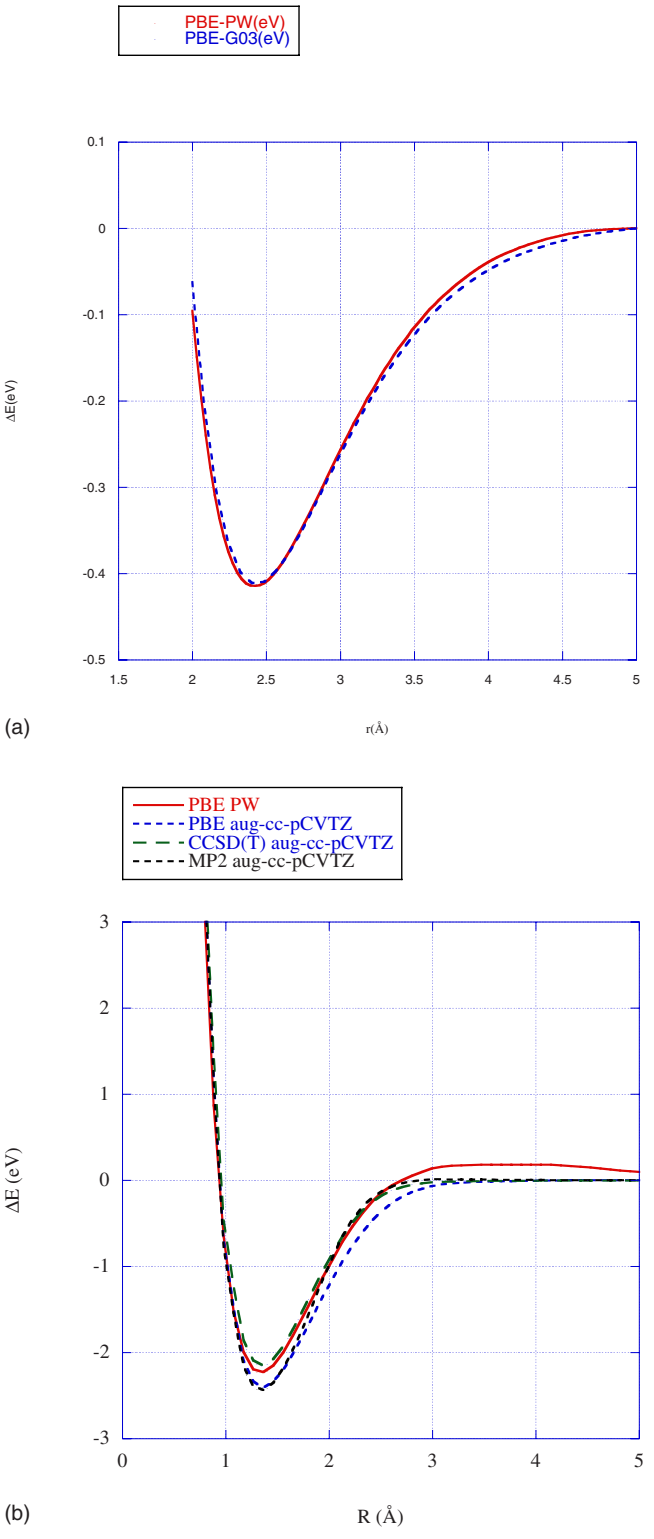

FIG. 1. (Color online) Quantum interatomic potentials. (a) Comparison of Be-Be interatomic potential Vanderbilt pseudopotential +plane wave basis orbital (solid line) and all-electron calculation PBE functional+aug-cc-pCVTZ basis set (broken line). (b) Comparison of Be-H interatomic potential, in solid line: Vanderbilt pseudopotential+plane wave basis orbital and in broken lines: all-electron calculation using aug-cc-pCVTZ basis set+PBE, CCSD(t), and MP2 methods

III. HYDROGEN BERYLLIUM INTERACTION

A. Single hydrogen atom on beryllium

The crystal supercell used for H/Be interaction is shown in Fig. 2(a). Two models are developed in agreement with

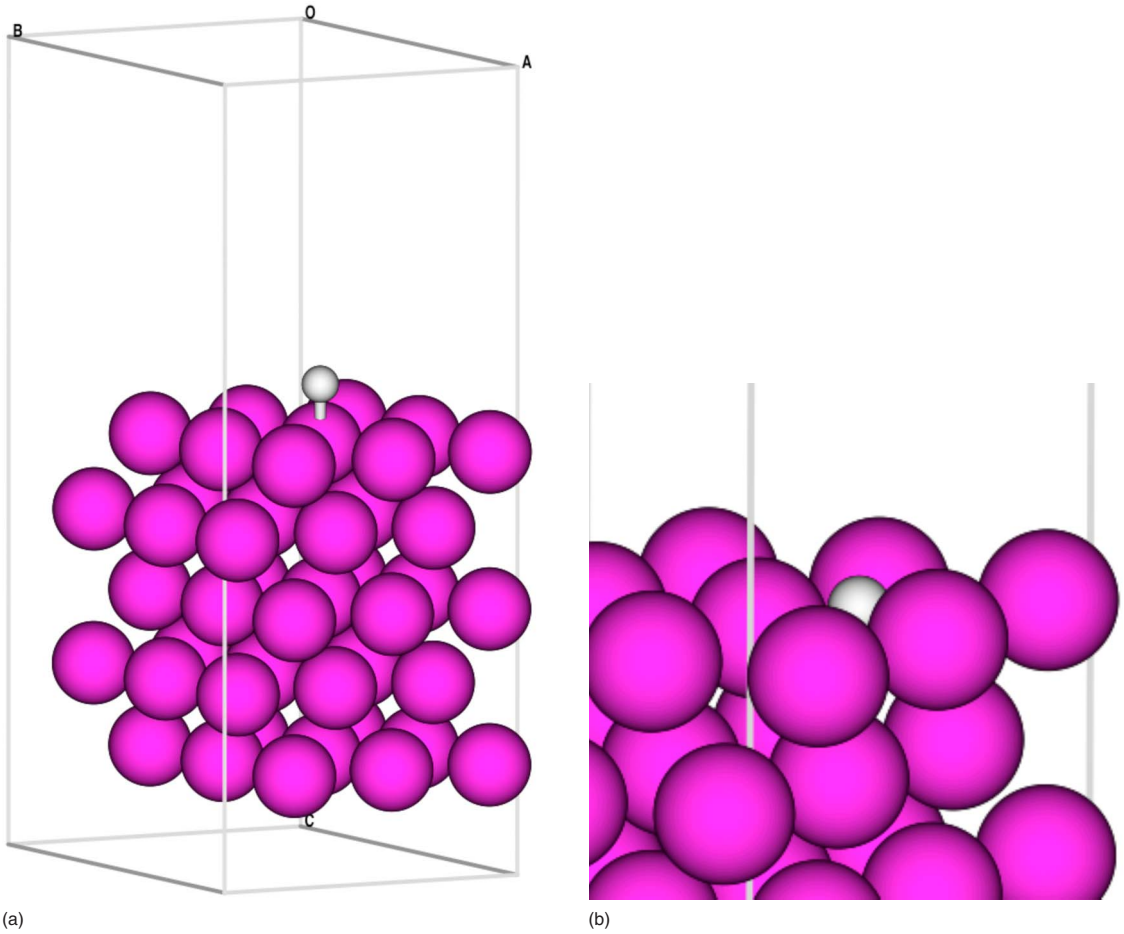

FIG. 2. (Color online) Single hydrogen adsorption on Be(0001) surface. (a) Beryllium working supercell studying interaction of a single hydrogen atom with the (0001) surface and atop H adsorption site. (b) Structure corresponding to the minimum energy bridge position.

the previously published works and two potential energy surfaces (PES) are associated to these models. A PES is associated (in the present case) to one coordinate[20] [the reaction coordinate (RC)]. In this section the most natural RC is H_z: the hydrogen altitude above the beryllium surface. H_z is scanned starting from an altitude high enough above the surface to have negligible H-Be interaction: this is the reference energy. All the other coordinates are fully optimized without any constraint of symmetry. The representation of the thus calculated energies vs H_z exhibits two kinds of stationary points corresponding to zero derivative: the local minimums and the transition states corresponding to the barrier the system has to overcome in order to evolve from one minimum to another one. In this paragraph the PESs (not represented) are calculated in order to determine the possible adsorption sites. Two models are selected: (1) H approaches the surface right above a surface atom (atop position), in which its three coordinates H_x, H_y, and H_z are fixed for each point of the PES; all the beryllium are able to relax. The minimum in energy is found for a Be-H distance of 1.37 Å [Fig. 2(a)] and an interaction energy of −1.51 eV. This process has little influence on the surface structure; the adsorption energy is noticeably smaller to those reported on Fig. 1(b) (−2.23 eV) while the bond length remains equivalent (1.33 Å) at the same level of approximation. (2) H approaches the surface according to an optimized trajectory: H_z is fixed but the other two coordinates are optimized. The deepest minimum occurs when H is only 0.85 Å above the original surface level, at equal distance (1.42 Å) from three superficial atoms [Fig. 2(b)]. The associated ΔE is equivalent to the dimer's one: −2.35 eV. Comparison between this value and the former one evidences that, although atomic beryllium is almost "spherical," its configuration is different when embedded in the crystal. The electronic density is noticeably lower in the direction normal to the surface than in the surface plane, and the hydrogen atom is more bonded to three equivalent Be and almost in the surface plane than right above a Be.

B. Hydrogenation of the Be(0001) surface

The hydrogen adsorption energy is calculated using Eq. (1) and without modifying the unit-cell parameters given in Sec. II. Surface coverage completion is reached when 12 H are adsorbed on the surface that includes nine Be atoms; adding an extra H would give molecular hydrogen since the next point in the PES would reach the domain of desorption barrier (~1 eV). This structure is referred to as the monolayer (ML) in the following.

On Fig. 3(a), the adsorption energy follows a quasiparabolic law at low coverage τ_H and the values are comparable

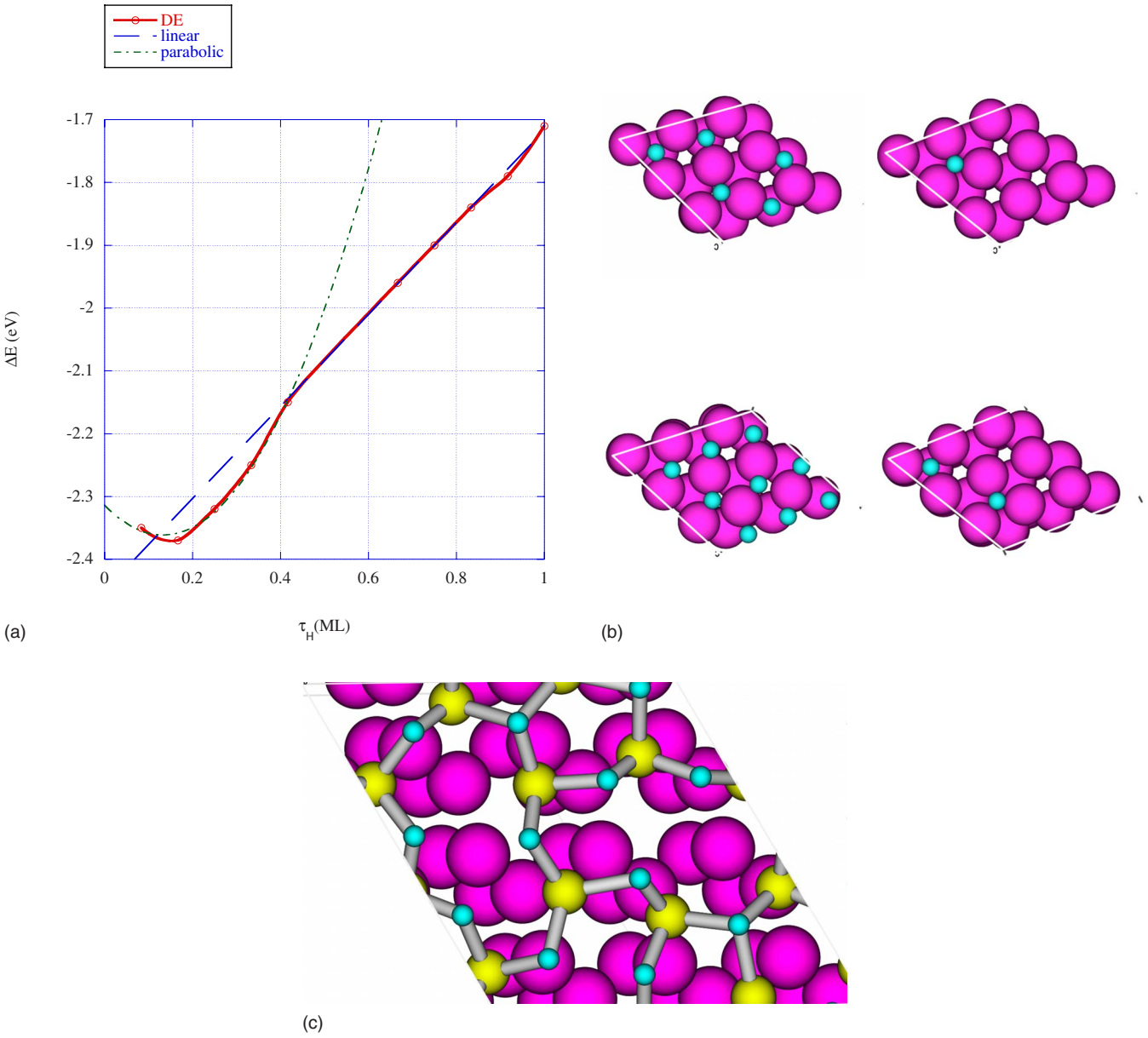

FIG. 3. (Color online) Hydrogen adsorption on Be(0001) vs surface coverage. (a) Adsorption energy (per H atom) and the ML corresponds to the ratio 12H/9Be. (b) Structure of adsorbed layers of special interest in space filling representation: 1H, 2H, 5H (0.42 ML), and 9H (0.75 ML) on the nine Be surface; no chemical bond is visible since all the Be-H distances are larger than 1.5 Å. (c) Structure of the H complete monolayer (12H/9Be) in ball and sticks representation; the Be surface atoms are in lighter color and the Be-H distances shorter than 1.5 Å are materialized.

to the BeH dimer as shown in Fig. 1(b). In this domain, each H is linked to two beryllium atoms at distances of about 1.5 Å.

For τ_H larger than 0.6 ML, the adsorption energy grows almost linearly up to −1.7 eV. This signifies that the lateral H-H interactions are negligible in the first domain whereas the vertical interactions have the best efficiency around 0.21 ML where the adsorption energy is −2.37 eV. At coverage larger than 0.6 ML, the lateral repulsions become predominant since the adsorption is less energetic than for a single adatom. In a first approximation, these repulsive contributions can be considered as mainly due to electrostatic interaction. Hydrogen atom adsorption implicates a charge transfer from the adatom to the substrate. In atop position, the H net charge (Löwdin definition) is 0.20 electron; it is slightly smaller in the bridge position (0.16 electron). This value does not change significantly for the higher hydrogen atom concentration on the surface; it goes from 0.10–0.16 electron at coverage corresponding to the angular point in Fig. 4(a) to 0.11–0.17 electron in the monolayer. In the same time, the average distance between first neighboring hydrogens decreases from 2.29 to 1.844 Å since the electrostatic repulsion grows as the inverse of the square of the internuclear distance; the repulsive part of the H-H interaction increases considerably.

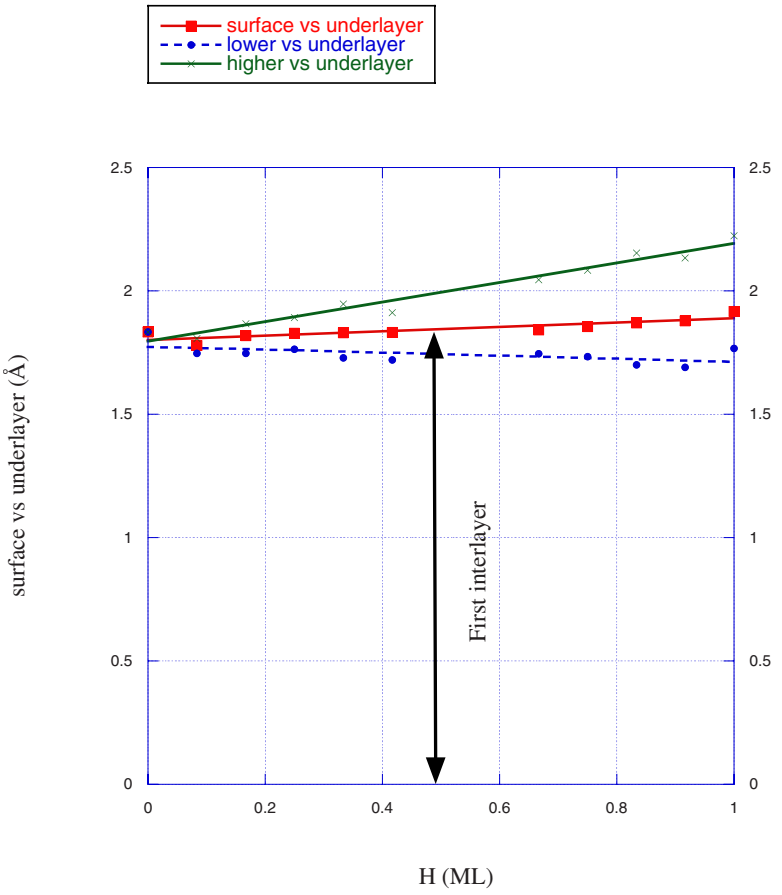

FIG. 4. (Color online) Be(0001) surface perturbation vs hydrogen coverage. In displacement of the surface atom compared to the bare surface level, the first underlayer is taken as the origin.

In Fig. 3(b), the hydrogen atoms organization is detailed for the most noteworthy undercompletion coverage structures. It can be observed at first sight that hydrogen never adopts the atop structure. It must be also remarked that, in the two H structure, the two atoms are not occupying vicinal positions because of the repulsive lateral interaction.

The monolayer corresponds to the ratio of 12H/9Be(surface). Each beryllium atom on the surface is surrounded by three hydrogens at distances ranging from 1.34 to 1.50 Å [Fig. 3(c)]. It can also be observed that at high coverage all the adsorption sites are bridge-type sites. Of course, this is only valid in the conditions of this DFT calculation: temperature is 0 K and no zero point energy correction. Taking account of the thermodynamics, the atoplike positions could have a nonzero probability.

Also from thermodynamics considerations, Stumpf and Feibelman[12] affirmed that the high coverage phases should be unstable against adsorption compared to molecular hydrogen formation. According to these authors, the thermodynamic saturation coverage is reached when the differential adsorption energy,

$$E_{\mathrm{ad}} = \Delta E(\tau_{\mathrm{H}}) + \tau_{\mathrm{H}} \frac{\delta[\Delta E(\tau_{\mathrm{H}})]}{\delta \tau_{\mathrm{H}}}, \tag{2}$$

is smaller than half the H_2 binding energy. If the function in Fig. 3(a) is numerically derived and if we select the value for H_2 (4.56 eV) calculated using PBE-PW at the same level of theory, Eq. (2) indicates that the adsorbed phase should be thermodynamically stable up to a coverage value of 0.49. It happens that this corresponds almost exactly to intersection point of the linear and parabolic regimes in Fig. 3(a). This should not be fortuitous: in this configuration, the H-H repulsion are so strong that formation of the molecule should be more energetic.

In order to compare our adsorption energies to thermal desorption spectroscopy (TDS) results, we have performed nudged elastic band (NEB) calculation[21–23] of the quantum barrier of activation of molecular hydrogen desorption from two of our model structures. For that we have selected five image configurations starting from two H adsorbed in neighboring sites and then their altitudes above the surface have been increased. Meanwhile the H-H distance was decreasing to reach the molecular atomic distance (0.7525 Å) 5 Å above the surface.

When two hydrogen atoms are adsorbed alone on two neighboring sites, the barrier is 1.11 eV and of course no diffusion process is to be considered; this value is slightly larger than the given experimental one. However, the barrier for two neighboring adatoms desorption from the structure at coverage around 0.4 ML [Fig. 3(b)] is only 0.90 eV. Since, at this coverage rate, the activation barrier to diffusion from one adsorption site to its equivalent one is only 0.51 eV, there is no competition with diffusion, i.e., molecular recombination is the dominant process, and it determines the barrier of activation to desorption. These results exhibit also the catalytic action of the substrate since the atomic desorption of two hydrogen would cost 2×2.37 eV=4.74 eV.

During hydrogenation, the metal surface undergoes some relaxation. Since the working system dimension is so small (for obvious technical reasons), only the two upper layers are described in this paragraph. On Fig. 4 are shown the superficial atom displacement with respect to the first underlayer. The average interlayer distance remains almost insensitive to hydrogen adsorption, the averaged values of the surface and first underlayer altitudes being shifted down with almost the same amplitude (0.07 and 0.04 Å). The larger upward (toward the vacuum) shift of the surface beryllium atoms is 0.39 Å, the larger downward (toward the bulk) displacement if only 0.07, and these evolutions are almost linear with surface coverage increasing. At monolayer completion, the hydrogen layer distance to the average metal surface level is included between 0.75 and 1.05 Å. Because the optimization of the various structures presented here has been done without any symmetry imposition, it is hardly possible to draw any general conclusion on this point.

IV. DISCUSSION AND CONCLUSION

One of the first attempts of quantum study on hydrogen adsorption on beryllium surface was given by Yu and Lam[24] within the framework of first-principles DFT, plane waves, and Hedin-Lunqvist functional. Our results are in excellent agreement with theirs since they give adsorption energies of −2.39 eV on bridge position (our work: −2.35 eV) and −1.67 eV atop (our work: −1.5 eV). Their adsorption site structures are also very similar to ours.

Our values are comforted by Stumpf and Feibelman's[12] results, giving the growing adsorption energies versus coverage as −2.3 eV (1/12 ML), −1.9 eV (1/3 ML), and −1.7 eV (1 ML); no minimum is reported by these authors. This order of magnitude is corroborated in Ref. 11 where it also is indicated that the atop geometry is disfavored by 0.72 eV compared to bridge (0.65 eV here).

The papers by Feibelman and Stumpf discuss the structure of the $(\sqrt{3}\times\sqrt{3})R30$ hydrogen monolayer structure, derived in Ref. 25 from low-energy electron diffraction (LEED) *I-V* spectra. In this structure, three hydrogen atoms, exactly as in Fig. 3(c), surround all the superficial beryllium atoms. However, due to our optimization procedure, which does not preserve symmetry, and the small size of our system, it is not possible here to compare the organization of the vacancies on the surface. At monolayer completion, they indicate a relaxation of the first interlayer of 3% of the ideal spacing. The value corresponding to completion is 4% of the bare surface; it is comparable to Feibelman's LAPW value of 4.5%.[25]

Marino and Ermler[10] proposed multiconfiguration self-consistent-field (MCSCF) calculation on a Be_{45} cluster. The equilibrium H surface distance of 0.86 Å is similar to ours. Nevertheless, they found a barrier of 0.53 eV before H adsorbs on a Be cluster of symmetry D_{3h}, which we did not; this can be explained by the nonoptimization of their surface. Then, the same authors propose various values for the adsorption energy: −0.42 eV (pure spin triplet), −3.05 eV (pure singlet), and −2.2 eV (average). They conclude to a barrier for recombination desorption of −0.86 eV in selecting the lower states of $Be_{45}H_2(R_\infty)$ and $Be_{45}H_2(R_{eq})$, which is in good agreement with the experimental TDS values by Ray *et al.*[26] that range from 0.7 to 1.2 eV.

Another TDS experiment was proposed afterward by Lossev and Küppers[27] on clean and oxygen-covered Be(0001) surface. Molecular H_2 desorption is observed to follow a second-order rate on clean surface and occurs at 450K, which corresponds to a desorption activation barrier of 0.87 eV, very close to our calculated value (0.90 eV).

However, beryllium, and the beryllium-hydrogen interaction, nowadays finds an interest because of its application planned in tokamaks. This work is intended to take part in the general discussion of beryllium implementation in the future tokamak ITER; therefore the major motivation is to compare beryllium and graphite in this context with the subjacent question: can quantum theory provide information on the crucial problem of hydrogen retention in the fusion device first wall cladding?

The first result of the former sections is that the H adsorption energy on Be is noticeably higher than on graphite [2.35 eV compared to 0.7 eV (Ref. 28)]; nonetheless this last value increases significantly at higher graphite surface coverage[29] to reach the same order of magnitude at completion. This data correlated with the special structure of the beryllium surface ensure coverage that is three times larger (1.33 H /Be at) compared to graphite (0.4 H /Be at). Actually, experiments in JET (Joint European Torus) tokamak (Ref. 30) show that the amount of deuterium required to fuel the tokamak during the beryllium phase was higher than for the carbon phase and it was suggested that surface effects drove the retention.

The better point is that the metal surface seems less sensitive to hydrogen adsorption in opposition with graphite, which is dramatically perturbed by these kinds of processes.[4] This must be correlated with the low desorption barrier and very easy diffusion on beryllium that ensure a better restitution of trapped hydrogen.

In conclusion, the first-principles calculation proposed in this paper has been able to explain without any empirical approximation the main features of hydrogen (deuterium) trapping in beryllium, as far as the surface is involved. The various interaction energies we calculated proved to be in good agreement both with experiment and other quantum works. We show that the hydrogen diffusion in this material is very easy and, from the models we proposed for adsorption processes, it can be concluded that hydrogen retention in beryllium could be significantly larger than in graphite but restitution is much more easy

ACKNOWLEDGMENTS

The author is very grateful to Ch. Linsmeier for many very fruitful discussions. This work is supported by the Euratom–CEA Association, in the framework of the Fédération de Recherche Fusion par Confinement Magnétique, and by the Agence Nationale de la Recherche (ANR CAMITER N° Contract No. ANR-06-BLAN-0008-01). The calculations were performed at the CEA (CCRT) and CNRS (IDRIS) computing Centers.

*alain.allouche@univ-provence.fr

[1] J. Wesson, *Tokamaks* (Oxford Science, Oxford, 2004).
[2] R. A. Causey, J. Nucl. Mater. **300**, 91 (2002).
[3] E. Abramov, M. P. Riehm, D. A. Thompson, and W. W. Smelter, J. Nucl. Mater. **175**, 90 (1990).
[4] Y. Ferro and A. Allouche, *Quantum Chemical Calculations of Surfaces and Interfaces of Materials*, edited by V. A. Basiuk and P. Ugliengo (American Scientific, Stevenson Ranch, CA, 2008).
[5] J. Roth, E. Tsitrone, and A. Loarte, Nucl. Instrum. Methods Phys. Res. B **258**, 253 (2007).
[6] R. P. Doerner, J. Nucl. Mater. **363**, 32 (2007).
[7] M. Reinelt and C. Linsmeier, Phys. Scr., T **128**, 111 (2007).
[8] P. Vajeeson, P. Ravindran, A. Kjekshus, and H. Fjellvag, Appl. Phys. Lett. **84**, 34 (2004).
[9] S. Sampath, A. I. Kolesnikov, K. M. Lantzky, and J. L. Yarger, J. Chem. Phys. **128**, 134512 (2008).
[10] M. M. Marino and W. C. Ermler, J. Chem. Phys. **94**, 8021 (1991).
[11] P. J. Feibelman, Phys. Rev. B **48**, 11270 (1993).
[12] R. Stumpf and P. J. Feibelman, Phys. Rev. B **51**, 13748 (1995).
[13] R. Stumpf, Phys. Rev. B **53**, R4253 (1996).
[14] L. G. Hector, J. F. Herbst, W. Wolf, P. Saxe, and G. Kresse, Phys. Rev. B **76**, 014121 (2007).
[15] A. Allouche and C. Linsmeier, J. Phys.: Conf. Ser. **117**, 012002 (2008).
[16] S. Scandolo, P. Giannozzi, C. Cavazzoni, S. de Gironcoli, A. Pasquarello, and S. Baroni, Z. Kristallogr. **220**, 574 (2005); Quantum Espresso website http://www.quantum-espresso.org
[17] E. Wachowicz and A. Kiejna, J. Phys.: Condens. Matter **13**, 10767 (2001).
[18] M. Lazzeri and S. de Gironcoli, Surf. Sci. **454-456**, 442 (2000).
[19] N. A. W. Holzwarth and Y. Zeng, Phys. Rev. B **51**, 13653 (1995).
[20] P. W. Atkins and R. S. Fridedman, *Molecular Quantum Mechanics*, 3rd ed. (Oxford University Press, New York, 1997).
[21] W. E, W. Ren, and E. Vanden-Eijnden, Phys. Rev. B **66**, 052301 (2002).
[22] Y. Kanai, A. Tilocca, A. Selloni, and R. Car, J. Chem. Phys. **121**, 3359 (2004).
[23] G. Henkelman and H. Jonsson, J. Chem. Phys. **111**, 7010 (1999).
[24] R. Yu and P. K. Lam, Phys. Rev. B **39**, 5035 (1989).
[25] P. J. Feibelman, Phys. Rev. B **46**, 2532 (1992).
[26] K. B. Ray, J. B. Hannon, and E. W. Plummer, Chem. Phys. Lett. **171**, 469 (1990).
[27] V. Lossev and J. Küppers, Surf. Sci. **284**, 175 (1993).
[28] Y. Ferro, F. Marinelli, and A. Allouche, J. Chem. Phys. **116**, 8124 (2002).
[29] A. Allouche, A. Jelea, F. Marinelli, and Y. Ferro, Phys. Scr., T **124**, 91 (2006).
[30] G. Saibene, R. Sartori, A. Tanga, A. Peacock, M. Pick, and P. Gaze, J. Nucl. Mater. **176-177**, 624 (1990).